Heterogeneous Interactions of HOBr, HNO_3, O_3, and NO_2 with Deliquescent NaCl Aerosols at Room Temperature

J. P. D. Abbatt* and G. C. G. Waschewsky

Department of the Geophysical Sciences, The University of Chicago, 5734 South Ellis Ave., Chicago, Illinois 60637

Received: January 28, 1998; In Final Form: March 18, 1998

To better quantify the rates at which key trace gases interact with sea-salt aerosols, the kinetics of uptake of HOBr, HNO_3, O_3, and NO_2 by deliquescent NaCl aerosols at 75% relative humidity (RH) and room temperature have been studied using an aerosol kinetics flow tube technique. Results for HOBr indicate that the uptake coefficient (γ) is larger than 0.2 for highly acidic aerosols at pH 0.3 and for aerosols that have been buffered to pH 7.2 using a 0.25 M NaH_2PO_4/Na_2HPO_4 buffer. For unbuffered NaCl aerosols, the HOBr uptake coefficient due to reaction is less than 1.5×10^{-3}. For HNO_3, the uptake coefficient on unbuffered, NaCl aerosols is greater than 0.2, being driven by the very high solubility of HNO_3 in aqueous salt solutions. Both NO_2 and O_3 show low reactivity on pH neutral aerosols with upper limits to the uptake coefficients of 10^{-4}. With acidic aerosols, slight O_3 loss occurs either on the walls of the flow tube or on the aerosols, giving rise to Cl_2. These experiments are the first reported kinetics studies of the loss of HOBr, HNO_3, and O_3 on aqueous NaCl solutions, and they imply that gas-phase diffusion, and not reaction kinetics, determines the mass-transfer rates of gas-phase HNO_3 and HOBr to marine aerosols in the boundary layer. Also, the HOBr results support modeling studies which have proposed that HOBr uptake initiates autocatalytic release of bromide from sea-salt aerosols.

Introduction

Recent field observations imply that substantial photochemical activity of halogen species can occur in the marine boundary layer. In particular, in the high Arctic springtime there is good evidence for enhanced levels of both bromine and chlorine free radicals which result in unusually high loss rates for ozone and reactive hydrocarbons, respectively.[1,2] A number of mechanisms involving heterogeneous chemistry of sea-salt aerosols have been proposed to explain the high levels of active halogens.[3−7] Although it has been less convincingly demonstrated, it is also possible that similar heterogeneous processes occur at lower latitudes, where high levels of gas-phase inorganic chlorine in a form different from HCl have been observed.[8] The full significance of this chemistry to the oxidizing capacity of the boundary layer on a global scale has yet to be fully determined and is the topic of much research.

Prompted by these observations, there has been considerable recent interest in determining the mechanisms and kinetics of reactions that can liberate chlorine from marine aerosol particles in order to better determine the dominant oxidants which exist within the marine boundary layer. Although it has long been known that acid-displacement processes such as (1) and (2) are important in this regard,[9−14]

$$HNO_3 + NaCl \rightarrow NaNO_3 + HCl \quad (1)$$

$$H_2SO_4 + 2NaCl \rightarrow Na_2SO_4 + 2HCl \quad (2)$$

it is now apparent that reactions involving nitrogen oxide species may also occur:[9,11,13−24]

$$2NO_2 + NaCl \rightarrow NaNO_3 + ClNO \quad (3)$$

$$N_2O_5 + NaCl \rightarrow ClNO_2 + NaNO_3 \quad (4)$$

$$NO_3 + NaCl \rightarrow NaNO_3 + Cl \quad (5)$$

These reactions involving members of the NO_x family are likely to be of most importance in regions where marine air interacts with polluted environments, as occurs off the California coast and the eastern seaboard of the United States. They are also of interest because the chlorine is significantly oxidized and in some cases released from the aerosol in a form more easily photochemically activated than is the HCl product of reactions 1 and 2.

Most recently, it has been suggested that halogen species themselves may participate in the release of sea-salt halogens via autocatalytic processes.[6,25,26] In particular, the effects that an autocatalytic release of bromine, initiated by the uptake of HOBr by a marine aerosol, may have upon the chemistry of the marine boundary layer have been modeled:[25]

* To whom correspondence should be sent.

S1089-5639(98)00932-3 CCC: $15.00
Published on Web 04/28/1998

$$HOBr + Cl^- + H^+ \rightarrow BrCl + H_2O \quad (6)$$

$$BrCl + Br^- \rightarrow Br_2Cl^- \quad (7)$$

$$Br_2Cl^- \rightarrow Br_2 + Cl^- \quad (8)$$

$$Br_2 + h\nu \rightarrow 2Br \quad (9)$$

$$[Br + O_3 \rightarrow BrO + O_2] \times 2 \quad (10)$$

$$[BrO + HO_2 \rightarrow HOBr + O_2] \times 2 \quad (11)$$

$$\text{net:} \quad Br^- + 2O_3 + 2HO_2 + H^+ \rightarrow H_2O + HOBr + 4O_2$$

Once this mechanism is initiated, it has the potential to oxidize essentially all of the bromide within marine boundary layer aerosols in a matter of a few days. Significant chemical effects, which include sizable destruction of ozone and oxidation of CH_3SCH_3 and SO_2, also arise as a result of the activation of bromine via this mechanism. The connection of this autocatalytic process to the surge of bromine that is regularly detected in the high Arctic springtime has yet to be definitively established, but it has been suggested that HOBr interactions with sea salt sprayed onto the sea-ice surface may be significant.[7] This reaction sequence also has the potential to lead to a small amount of chlorine activation, via outgassing from the sea-salt aerosol of a fraction of the BrCl product formed in reaction 6.[25]

In this paper we present kinetics studies of the interactions of four trace gases—HOBr, HNO_3, NO_2, and O_3—with deliquescent sodium chloride aerosols at 75% relative humidity and room temperature. These specific environmental conditions were chosen to resemble those routinely encountered in the marine boundary layer. Previous studies have already demonstrated that HOBr is reactive toward both HBr and HCl, when dissolved in sulfate aerosols or adsorbed to ice.[27−30] In addition, it has been shown that both BrCl and Br_2 are liberated when a frozen solution of the composition of seawater is exposed to gas-phase HOBr.[31] However, this work represents the first investigation of HOBr interactions with aqueous sodium chloride solutions, i.e., with salt aerosols of the phase expected to be prevalent under the high relative humidity conditions of the marine boundary layer.

In the case of HNO_3, O_3, and NO_2, there have been a number of previous studies involving solid NaCl substrates,[9−18] including experiments that have demonstrated the importance of adsorbed water to the rate of HNO_3 uptake (as in ref 13, for example). However, as with HOBr, these are also the first reported uptake coefficient measurements for the interactions of HNO_3 and O_3 with deliquescent NaCl aerosols. With respect to the interaction between aqueous NaCl aerosols and NO_2, there has been one previous study: Behnke et al. report low reactivity, measuring an upper limit to the uptake coefficient of 10^{-4}.[19]

Experimental Section

All the uptake experiments were conducted using an aerosol kinetics flow tube which has been fully described in a previous publication where the kinetics of the loss of N_2O_5 on aqueous sulfuric acid aerosols at room temperature were studied.[32] The close agreement between our measurements and those of a number of other groups[33−37] for the N_2O_5 uptake coefficients at low relative humidities gives us confidence that this relatively new experimental system can perform accurate kinetics measurements. The following is a brief description of the technique, along with details that are specific to the experiments performed in this work. A schematic diagram is shown in Figure 1.

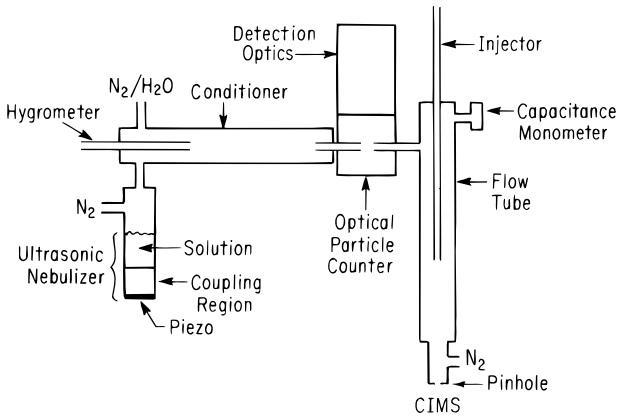

Figure 1. Schematic diagram of the experimental apparatus.

Aqueous sodium chloride aerosol particles are formed from a concentrated salt solution (4−5 M) using a home-built ultrasonic nebulizer. A small flow of nitrogen (10−100 sccm) carries particles at room temperature to a conditioning flow tube where they are mixed with a much larger flow of nitrogen (2000−2200 sccm) which is at a relative humidity of 75%, the deliquescence point of sodium chloride.[38,39] This larger nitrogen flow is prepared by mixing together a dry nitrogen flow and a flow that has passed through a water bubbler. The relative humidity calculated to arise in the flow tube equals that measured by a hygrometer (Fisher Scientific) to ±3% RH. The salt concentration of the aerosols does not change substantially in going from the nebulizer source to the conditioning flow tube, since the composition of the sodium chloride solution from which the aerosols are formed is very similar to the composition of NaCl aerosols at the deliquescence point (5.3 M).[38,39] For reasons described in the Atmospheric Implications section, all the aerosol particles are thought to be liquid.

After spending 6 s in the conditioning flow tube, the combined flow passes through an optical particle counter (Particle Measuring Instruments, Inc., model SSIP-S2), where the aerosol particles are sized and their number density is determined. The counting accuracy of the optical particle counter is on the order of ±10%. Using latex spheres of known diameter, the sizing accuracy of the instrument for latex is confirmed to be 10−15%. Since the refractive index of the liquid NaCl particles is somewhat lower than that of latex, the optical particle counter undersizes NaCl aerosols, and the sizes measured by the optical particle counter must be corrected using an empirically determined correction factor. As described in detail in Hu and Abbatt,[32] this factor is determined from the ratio of the moles of NaCl solute measured by the optical particle counter (as calculated from the molarity of the particles and the total measured aerosol volume) for aerosols flowing through the system at a known relative humidity to the moles of solute determined by electrical conductivity measurements of a solution that traps all the particles flowing through the counter during a fixed period of time. The cube root of this ratio is the correction factor which is applied to the particle sizes measured by the optical particle counter. Although a bimodal distribution of both large (average diameter from 2 to 4 μm) and small (diameter less 1 μm) particles are formed by the nebulizer (see ref 32 for typical log-normal distributions), those in the range of 1−5 μm diameter provide over 95% of the total aerosol surface area in the flow tube. Typical total surface areas and number densities of the large particles in the flow tube are 1×10^{-3} to 6×10^{-3} cm^2/cm^3 and 1×10^4 to 4×10^4 particles/cm^3, respectively.

From the optical particle counter, the flow passes into the upstream end of a 90 cm long, 3.0 cm i.d. room-temperature kinetics flow tube, where uptake experiments are performed in the standard manner by monitoring the decay of a gas-phase molecule as a function of the position of an axial injector through which the reactive species is being added to the flow. The total pressure in the flow tube is 700−760 Torr, and the bulk flow velocity is approximately 6.0 cm/s. The gas-phase composition is monitored using a chemical ionization mass spectrometer (CIMS), connected to the flow tube at the downstream end by a pinhole in a Teflon sheet mounted in a Cajon vacuum fitting. When working with salt particles, as opposed to aqueous sulfuric acid aerosols, there is a tendency for small apertures to become easily clogged with salt via aerosol deposition. This problem arose frequently with small pinholes, and to circumvent it, we added one of the large carrier gas flows (≈8 SLPM N_2) used in the CIMS source immediately upstream of the pinhole connecting the flow tube to the CIMS source (see Figure 1). So doing does not affect the flow of gases within the kinetics flow tube, and it allows for a much larger, less easily plugged pinhole to be used.

Within the CIMS source, an additional flow of N_2 (≈8 SLPM) containing a trace amount of SF_6 passes through a Po-210 radioactive source to create SF_6^- ions. This flow of reagent ions is then mixed with the flow of gas coming in from the kinetics flow tube. En route from the CIMS source to the quadrupole mass spectrometer, ions from this combined flow then pass through three stages of differential pumping, which includes an ion declustering region at 1 Torr.[40] The pinholes that separate the different stages of pumping are all negatively biased, with the most neutral located closest to the quadrupole.

Via a number of well-studied ion−molecule reactions,[41] SF_6^- is used to detect the following species: HOBr as SF_5O^-, Br_2O as FBr_2O^-, BrCl as $BrCl^-$, Cl_2 as Cl_2^-, HNO_3 as NO_3^-, HCl as SF_5Cl^-, O_3 as O_3^-, and NO_2 as NO_2^-. Detection limits for gases in the kinetics flow tube are higher than for those in the CIMS source because of the significant dilution that occurs with the addition of the CIMS carrier gases. Nevertheless, for HOBr, NO_2, and O_3, typical values for the detection limit (S/N = 1, 5 s integration) are on the order of 6×10^9 to 6×10^{10} molecules/cm^3, with the range reflecting the different rate constants for the ion−molecule reactions with SF_6^-. For HNO_3, the detection limit is somewhat higher, approximately 3×10^{11} molecules/cm^3, because of a significant background signal arising from the flow tube at the mass used to detect NO_3^- (see below). The kinetics experiments were performed so that there was no detectable change in the SF_6^- signal during a decay, thus ensuring a linear response.

The decays of reactive gases as a function of injector position are measured for a range of total aerosol surface areas (A) in the flow tube. The decays are converted to first-order rate constants (k^I) using the bulk flow velocity and the standard correction for non-plug-flow conditions.[42] An uptake coefficient (γ) is calculated from each first-order rate constant using eq 12:[43]

$$k^I = \frac{\gamma A v}{4 + \frac{3\gamma(1 + 0.38K_n)}{K_n(1 + K_n)}} \qquad (12)$$

where K_n, the Knudsen number, equals $6D_g/dv$, and D_g is the gas-phase diffusion coefficient of the reactive gas, d is the aerosol diameter, and v is the mean molecular velocity. Values of the diffusion coefficients were calculated to be 0.125 cm^2/s for HOBr and 0.135 cm^2/s for HNO_3.[44] Equation 12 is strictly only fully correct for a monodisperse distribution of aerosols. For the polydisperse aerosol used in our experiments, we have shown in an earlier publication that the equation is accurate to at least 5% when we take the aerosol diameter to be at the maximum of the surface area distribution of the larger aerosols present in the flow tube.[32]

The uptake coefficient is proportional to the first-order rate constant when its value is small. However, when the uptake coefficient becomes large, gas-phase diffusion limits to some extent the rate of mass transfer of molecules from the gas phase to the surface of the aerosols. For the total flow tube pressure and the average aerosol diameters of approximately 3 μm, the largest uptake coefficient that can be reliably measured in our system is 0.2. That is, for the fastest decays that we observe in the flow tube, the measured first-order rate constants correspond to uptake coefficients with values somewhere between 0.2 and 1. This lower limit to the uptake coefficient is determined by using eq 12 to determine how the precision of the k^I measurements, and the total uncertainties estimated for the aerosol surface area (±25%), aerosol diameters (±10%), and gas-phase diffusion coefficients (±10%), may affect the calculated value of the uptake coefficient.

A variety of reactive gas sources were used for this work. To make HOBr, a steady-state trace flow of Br_2 was passed through a 1 cm i.d., 50 cm long glass tube that was loosely packed with a mixture of yellow mercuric oxide and 2 mm diameter glass beads.[45] The carrier gas for the Br_2 was 100 sccm N_2 at ≈70% relative humidity. The water is added to convert Br_2O, formed by the reaction of Br_2 with HgO, to HOBr:

$$Br_2O + H_2O \rightarrow 2HOBr \qquad (13)$$

In a separate experiment, where we have a similar HOBr source coupled to a UV absorption cell used to detect HOBr, we have determined that the conversion efficiency of Br_2 to HOBr is about 10%. Although we have not determined the conversion efficiency for the source used in the experiment described in this work, we believe that it is similar. After an initial time during which the HgO column must be conditioned each day, the HOBr source is stable and easy to use. Assuming a conversion efficiency of 10% and using measured Br_2 flow rates, the concentrations of HOBr within the kinetics flow tube are estimated to be on the order of 2×10^{12} to 1×10^{13} molecules/cm^3.

O_3 was delivered to the flow by passing a small flow of N_2 (5−10 sccm) through a trap filled with ozone adsorbed onto silica gel and held at the temperature of a dry ice−acetone bath. To prepare the ozone trap, a dry O_2 flow was passed through a UV−ozone source and then through the cold silica gel trap. Both NO_2 and HNO_3 were added to the flow tube from glass reservoirs, filled with a dilute mixture of these gases in nitrogen. HNO_3 was added to the reservoir by taking the vapor from a 3:1 solution of 96 wt % sulfuric acid and 70 wt % nitric acid solutions, which had been degassed via freeze−pump−thaw cycles.

Results and Discussion

1. Uptake of HOBr. Kinetics studies using unbuffered aerosols composed of aqueous sodium chloride showed extremely low reactivity with HOBr. As illustrated in Figure 2, where the observed first-order rate constants for HOBr decays are plotted versus aerosol surface area, there is little enhancement in the decay of HOBr above the wall-loss value measured

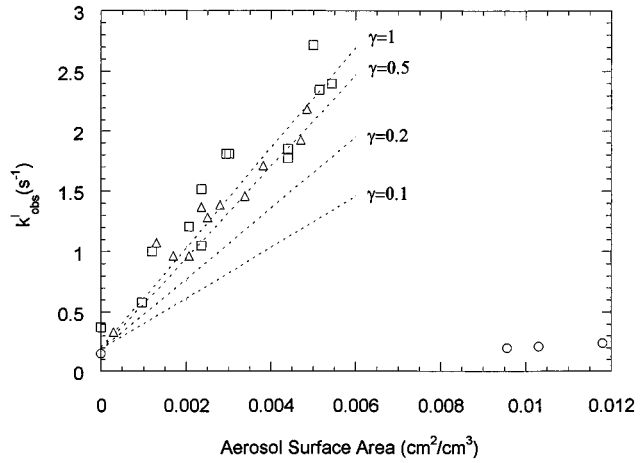

Figure 2. Observed first-order rate constants as a function of aerosol surface area for the loss of HOBr on deliquescent NaCl aerosols at 75% RH, 298 K. The symbols at zero surface area represent wall loss experiments conducted immediately after aerosols had been present in the flow tube. Circles, unbuffered aerosols; squares, pH 0.3 aerosols; triangles, pH 7.2 aerosols. For illustration sake, dotted lines indicate the calculated dependence of k^I upon aerosol surface area for different values of γ^{HOBr}, assuming typical experimental conditions.

in the absence of aerosols in the flow tube. From these measurements an upper limit to the uptake coefficient was determined to be 1.5×10^{-3}. However, when the aerosols are acidified to pH 0.3, there is a pronounced increase in the observed rate constant as a function of aerosol surface area (see Figure 2). The small intercept in the figure is presumably due to the reaction between HOBr and NaCl aerosols deposited to the flow tube walls. In this case, acidified aerosols were prepared by nebulizing a 5 M NaCl + 0.5 M HCl solution. Adding the HCl to the NaCl solution affected the concentration of the chloride ion to only a minor extent, whereas the hydrogen ion concentration was increased significantly.

The reason for the strong dependence of the HOBr reactivity on the acidity of the aerosols is clear. The concentration of HOBr in the gas phase, somewhere between 2×10^{12} and 1×10^{13} molecules/cm^3, is sufficient to readily deplete the initial supply of hydrogen ions, one of the reactants in reaction 6, present in the aerosols. Given that the initial hydrogen ion concentration in the unbuffered aerosols is approximately 10^{-7} M and that the total aerosol volumes present in the flow tube for kinetics studies are between 5×10^{-8} and 4×10^{-7} cm^3/cm^3, there are between 4×10^6 and 2.5×10^7 hydrogen ions present per cm^3 of carrier gas. This low concentration would be readily depleted by reacting with only a small fraction of the HOBr. The aerosols must then become alkaline, as water molecules dissociate to provide protons for the reaction. However, the overall rate of reaction 6 under these alkaline conditions must be sufficiently slow so as to give rise to the low upper limit to the uptake coefficient which is measured. To not significantly deplete the hydrogen ion concentration of unbuffered NaCl aerosols via reaction with HOBr would require operating with unrealistically low HOBr concentrations, many orders of magnitude smaller than those we are currently using. However, by adding high concentrations of HCl to the nebulizing solution, we can ensure that the hydrogen ion concentration in the aerosol particles is not significantly depleted via reaction with HOBr. In particular, for aerosols that are 0.5 M in hydrogen ion concentration, the number of protons available for reaction is between 2×10^{13} and 1×10^{14} per cm^3 of carrier gas, i.e., in excess of the HOBr concentrations in the flow tube.

The uptake coefficient that is calculated for the decays measured with pH 0.3 aerosols is between 0.2 and 1, i.e., at the limit at which we can measure loss of HOBr onto aerosols under the present experimental configuration. To more realistically simulate the pH of atmospheric sea-salt aerosols, the aerosols were buffered by adding 0.25 M of a weak acid and 0.25 M of its salt, in the forms of NaH_2PO_4 and Na_2HPO_4, to the nebulizing solution. Since the pK_a of $H_2PO_4^-$ is 7.2,[46] the pH of the aerosols was buffered to a value of 7.2 by mixing together equal concentrations of the two species. Note that the pH of 7.2 is valid unless the effects of the high ionic strength of the solution on the acid dissociation are significant. When kinetics experiments were performed with these aerosols, a clear dependence of the HOBr decays upon the aerosol surface area in the flow tube was observed. Within the precision of the measurements, the kinetics of HOBr loss are indistinguishable from those on pH 0.3 aerosols; i.e., the uptake coefficient for HOBr on NaCl aerosols that are buffered to pH 7.2 is between 0.2 and 1 at 75% relative humidity and room temperature.

As in all kinetics studies using pH buffers of this type, there is the possibility that the enhancement of the HOBr uptake on the buffered solutions is due to direct reaction with either the $H_2PO_4^-$ or HPO_4^{2-} ions, and not with H_3O^+. Indeed, there is good evidence from the kinetics studies of Margerum and coworkers that reactions of this form are general-acid-assisted.[47] The overall stoichiometry for the process is

$$HA + HOBr + Cl^- \rightarrow BrCl + H_2O + A^- \qquad (14)$$

where HA is a general acid such as H_3O^+ or $H_2PO_4^-$, which acts as a proton donor in the transition state of the reaction. At present there are no liquid-phase kinetics experiments which have been performed that allow us to determine whether the acid that is driving the reactivity in our pH 7.2 aerosols is H_3O^+ or $H_2PO_4^-$. To conclusively demonstrate that $H_2PO_4^-$ is acting as the proton donor in our experiments would require working with significantly lower HOBr gas-phase number densities and phosphate buffer concentrations. In particular, the $H_2PO_4^-$ ion could be shown to be the proton donor if it were observed that lower buffer concentrations lead to smaller uptake coefficients at constant pH.

Although either $H_2PO_4^-$ or H_3O^+ may be acting as the proton donor in our experiments, we are confident that the HPO_4^{2-} ion is not. When experiments were performed with aerosols formed from a NaCl solution that contained only 0.25 M Na_2HPO_4 and no NaH_2PO_4, there is observed to be no HOBr−aerosol reaction, and the kinetics are indistinguishable from those that were observed for the unbuffered NaCl aerosols. Similarly, no reaction is observed for aerosols buffered to pH 12.7, prepared by nebulizing a NaCl solution with 0.25 M Na_2HPO_4 (p$K_a(HPO_4^{2-}) = 12.7$)[46] and 0.25 M Na_3PO_4.

Two final points should be made. First, it is possible that at neutral pH the reaction could be proceeding via BrO^-, the anionic form of dissolved HOBr, and not via HOBr, as written in eqs 6 and 14. Since HOBr is a weak acid with a pK_a of 8.7,[48] it is calculated that 3% of dissolved HOBr is in the form of BrO^- and 97% is in the molecular form at pH 7.2. Thus, the reaction will proceed via BrO^- if the kinetics via that reactant are significantly faster than via dissolved HOBr. Such is the case for the reaction between dissolved HOCl and Br^-: the termolecular rate constant for the reaction of H_3O^+ and Br^- with ClO^- is over 4 orders of magnitude larger than the rate constant for reaction with HOCl.[47]

Second, it should be noted that it is possible for our experimental conditions that efficient dissolution of highly soluble gases by aqueous aerosols could lead to large observed

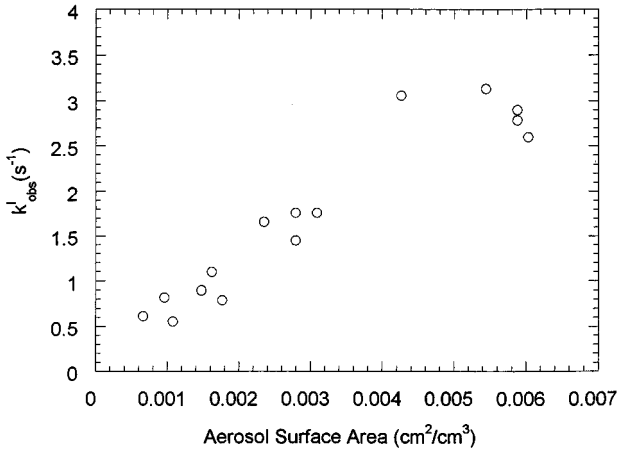

Figure 3. Observed first-order rate constants as a function of aerosol surface area for the loss of HNO_3 on deliquescent NaCl aerosols at 75% RH, 298 K.

uptake coefficients. However, the lack of HOBr uptake on unbuffered NaCl aerosols represents a control experiment which demonstrates that the loss of HOBr on acidified aerosols is driven by reactive processes and not by the solubility of HOBr in aqueous NaCl solutions.

2. Uptake of HNO_3. The dependence of the HNO_3 decay rate constant on the surface area of unbuffered aqueous NaCl aerosols is shown in Figure 3. As with HOBr loss on solutions of pH 0.3 and 7.2, the uptake coefficient calculated from the data in the figure is the largest that can be measured, i.e., $\gamma^{HNO_3} > 0.2$. Unlike the decays involving HOBr, the loss of HNO_3 on unbuffered NaCl aqueous aerosols is driven by the extremely high solubility of HNO_3 in aqueous solutions[49] and not by a reactive process involving the breaking and forming of covalent bonds with the Cl^- ion.

The concentrations of HNO_3 that were used in these experiments, 1×10^{13} to 2×10^{13} molecules/cm^3, were somewhat higher than the HOBr concentrations used because of a sizable background signal at mass 62, presumably originating from the nitric acid-containing aerosol which is formed in the reaction and then deposited to the flow tube walls. For each decay this background was determined by pulling the injector back to a point where the HNO_3 signal no longer declined as a function of injector position. When the HNO_3 flow was shut off, the background signal at mass 62 slowly decayed away, indicative of slow desorption of HNO_3 from the wall.

The nitric acid vapor pressure of the aerosols at the end of the decays can be calculated by using the Henry's law constant for HNO_3[49] and by assuming that all the HNO_3 is partitioned to the aerosol. For the smallest aerosol volumes used in this work, 5×10^{-8} cm^3/cm^3, the equilibrium gas-phase concentrations calculated for HNO_3 are very close to our HNO_3 detection limits, between 1×10^{11} and 4×10^{11} molecules/cm^3 for initial concentrations between 1×10^{13} and 2×10^{13} molecules/cm^3. For larger total aerosol volumes, the nitric acid vapor pressures are lower. Thus, we are able to perform this experiment because the solubility of HNO_3 is extremely high and because we use relatively large aerosol volumes. If either the solubility or the total aerosol volumes were very much smaller, then the aerosols would readily saturate with HNO_3, and no decays would be observed on the time scale of the experiment.

A large HCl background signal arose in the flow tube due to the uptake of HNO_3 by NaCl that had been deposited onto one of the wall surfaces present in the experiment. The background was sufficiently large that it did not allow us to detect the HCl gas-phase product formed via reaction 1. Increasing the initial concentration of HNO_3, in an attempt to increase the signal of HCl arising from the aerosols, was not successful since the background arising from the wall source increased as well.

3. Upake of NO_2. No statistically significant decay of the NO_2 signal was observed when NO_2 was given a long reaction time (≈8 s) in the presence of high total surface areas of unbuffered NaCl aerosols. An upper limit to the uptake coefficient was determined to be 1×10^{-4}, for NO_2 concentrations ranging from 3×10^{12} to 2×10^{14} molecules/cm^3. Similar experiments were conducted with NaCl aerosols buffered to pH 7.2 with the NaH_2PO_4/Na_2HPO_4 system and with aerosols set to pH 0.3 by the addition of HCl. In each case, the same upper limit to the uptake coefficient was calculated.

4. Uptake of O_3. No loss of ozone was detected in experiments performed on pH neutral aerosols. In particular, for both unbuffered aerosols and for pH 7.2 aerosols, an upper limit of 1×10^{-4} for the uptake coefficient of ozone was measured. Ozone concentrations were approximately 5×10^{11} to 1×10^{12} molecules/cm^3. For experiments involving pH 0.3 aerosols, which had been acidified by the addition of HCl to the NaCl nebulizing solution, a 5−10% decline in the ozone signal was detected for high aerosol surface areas (≈7×10^{-3} cm^2/cm^3) and long reaction times (≈8 s). Coincident with the decline in the ozone signal was an increase in the signal of Cl_2. If the reaction is occurring on the aerosols, this loss in signal corresponds to an uptake coefficient of 1×10^{-4} to 2×10^{-4}. However, as discussed below, it is more likely that the heterogeneous loss of ozone is occurring with aerosols and HCl that have been deposited onto the walls of the flow tube.

Atmospheric Implications

With respect to the atmospheric significance of the large uptake coefficient of HNO_3 measured in this work, it is concluded that the rate of the heterogeneous interaction of HNO_3 with marine aerosols at 75% relative humidity does not limit the overall rate of mass transfer of HNO_3 from the atmosphere to the condensed phase. In particular, for aerosols a few microns in diameter, gas-diffusion becomes rate limiting for uptake coefficients which are roughly 0.1 and larger.[43]

It should also be noted that our HNO_3 uptake coefficient is significantly larger than literature values for the uptake coefficients of HNO_3 on dry NaCl surfaces, which range in value from 10^{-4} to 10^{-2}, depending upon the extent of water on the salt surface.[10−14] Under the high relative humidity conditions usually present in the marine boundary layer, laboratory experiments imply that sea-salt aerosols will exist in the liquid state (see refs 50−52, for example). And so, we believe that our lower limit to the uptake coefficient is more accurate for modeling HNO_3−sea salt heterogeneous chemistry than those measured previously on solid NaCl surfaces. On a related topic, it should be noted that we are confident in this work that the aerosols in the flow tube are liquid solutions. The relative humidity in the flow tube is very close to the deliquescence point of NaCl, and it is well-known from a variety of experiments that aqueous NaCl aerosols do not readily crystallize, remaining in a supersaturated state down to relative humidities of between 40 and 45%.[51,52]

Our measurements of the large uptake coefficient for HOBr provide support for the validity of the HOBr-catalyzed, autocatalytic bromine release mechanism of Vogt, Crutzen, and Sander.[25] In particular, we can compare the measured value of the uptake coefficient for HOBr for reaction 6, believed to be the rate-determining step in the mechanism of reactions 6−11,

to a value calculated using eq 15:

$$\gamma^{HOBr} = \frac{4RTH^{HOBr}(D^{HOBr}k^{III}[H^+][Cl^-])^{1/2}}{v} \qquad (15)$$

Equation 15 describes the dependence of the uptake coefficient upon the chloride and hydrogen ion concentrations in marine aerosols, the termolecular, liquid-phase rate constant for the reaction (k^{III}), the Henry's law constant for HOBr (H^{HOBr}) in aqueous solutions, and the liquid-phase diffusion coefficient for HOBr (D^{HOBr}).[53] As written, eq 15 assumes that mass accommodation does not limit the uptake coefficient; i.e., it is assumed that the mass accommodation coefficient is close to unity, as it is has been measured to be for the loss of HOCl on dilute sulfuric acid aerosols at 251 K.[54] Our experiments show that the mass accommodation coefficient for the uptake of HOBr by concentrated aqueous salt aerosols is at least 0.2.

A lower limit of 5.6×10^9 M^{-2} s^{-1} in water has been determined for the termolecular rate constant for reaction 6,[25] whereas the only measurement for the Henry's law constant of HOBr gives a value of greater than 1.9×10^3 M/atm.[55] Using eq 15 and these lower limits to k^{III} and H^{HOBr}, it is calculated that the uptake coefficient is unity using typical atmospheric conditions: the aerosols are assumed to be 3 μm in radius, the pH is taken to be 7.2, the chloride ion concentration is 5.3 M (i.e., the value for NaCl aerosols at the deliquescence relative humidity), and the liquid-phase diffusion coefficient for HOBr is taken to be 3×10^{-5} cm^2/s.[56] The dependence of the size of the aerosol on the uptake coefficient has also been taken into consideration using the approach outlined in ref 57. Thus, the conclusion that can be made from this calculation is that our measurements are in agreement with the best value that can presently be calculated for the HOBr uptake coefficient for reaction 6, assuming that H_3O^+ is the acid acting as the proton donor in both the atmosphere and in our laboratory experiment.

As described above in the Results and Discussion section, additional kinetics experiments are required to conclusively determine whether the high reactivity that we observe for HOBr on pH 7.2 aerosols is due to reaction with H_3O^+ or with the $H_2PO_4^-$ ion present as part of the buffer system. In addition, it should also be pointed out that the kinetic role of general acids dissolved in true marine aerosols also needs to be examined to accurately determine the rate of reaction 6 under the most realistic atmospheric conditions. For example, the HCO_3^- ion is present at the millimolar level in seawater.[58]

Finally, in agreement with the study described in ref 19, no reaction was observed for the loss of NO_2 on either neutral or acidic salt aerosols. It is unlikely that the heterogeneous reactions of NO_2 on aqueous marine aerosols will be a significant source of active chlorine to the marine boundary layer, except perhaps in highly polluted environments. For ozone, interactions with pH neutral aerosols were also shown to be slow. However, for experiments involving acidic aerosols, a slow heterogeneous reaction was observed to occur with either the walls of the flow tube or on the aerosols themselves. Given that Cl_2 was observed to form, the net reaction that is destroying ozone is likely the following:

$$\text{net:} \quad O_3 + 2Cl^- + 2H^+ \rightarrow Cl_2 + H_2O + O_2 \qquad (16)$$

The rate expression for this overall process has been shown to have two contributions, one independent of the hydrogen ion concentration and one dependent upon it.[59] However, using the appropriate form for eq 15, we have calculated that the uptake coefficient for O_3 on deliquescent aerosols should be extremely small, $\gamma^{O_3} \approx 5 \times 10^{-8}$, even with high acidity aerosols of pH 0.3.[60] Thus, it seems most likely that the loss of ozone and the formation of Cl_2 is driven by a heterogeneous wall process and not via an aerosol reaction. Behnke and co-workers have arrived at a similar conclusion, when explaining observations of the formation of photolytically active chlorine formed in aerosol chamber kinetics studies involving NaCl particulates and O_3.[62] It should be noted that Oum et al. have recently observed the formation of molecular chlorine when mixtures of ozone and deliquescent NaCl aerosols are irradiated with 254 nm light.[63] In our case, it is likely that Cl_2 is being formed by a different mechanism at the molecular level since we observe that Cl_2 formation proceeds when all the lights in the laboratory are off.

Acknowledgment. Financial support for this work came from the Atmospheric Chemistry Program at the National Science Foundation.

References and Notes

(1) Barrie, L. A.; den Hartog, G.; Bottenheim, J. W.; Landsberger, S. *J. Atmos. Chem.* **1989**, *9*, 101.
(2) Jobson, B. T.; Niki, H.; Yokouchi, Y.; Bottenheim, J.; Hopper, F.; Leaitch, R. *J. Geophys. Res.* **1994**, *99*, 25355.
(3) Finlayson-Pitts, B. J.; Livingston, F. E.; Berko, H. N. *Nature* **1990**, *343*, 622.
(4) Fan, S.-M.; Jacob, D. J. *Nature* **1992**, *359*, 522.
(5) McConnell, J. C.; Henderson, G. S.; Barrie, L.; Bottenheim, J.; Niki, H.; Langford, C. H.; Templeton, E. M. J. *Nature* **1992**, *355*, 150.
(6) Mozurkewich, M. *J. Geophys. Res.* **1995**, *100*, 14199.
(7) Tang, T.; McConnell, J. C. *Geophys. Res. Lett.* **1996**, *23*, 2633.
(8) Pszenny, A. A. P.; Keene, W. C.; Jacob, D. J.; Fan, S.; Maben, J. R.; Zetwo, M. P.; Springer-Young, M.; Galloway, J. N. *Geophys. Res. Lett.* **1993**, *20*, 699.
(9) Robbins, R. C.; Cadle, R. D.; Eckhardt, D. L. *J. Meteorol.* **1959**, *16*, 53.
(10) Laux, J. M.; Hemminger, J. C.; Finlayson-Pitts, B. J. *Geophys. Res. Lett.* **1994**, *21*, 1623.
(11) Vogt, R.; Finlayson-Pitts, F. P. *J. Phys. Chem.* **1994**, *98*, 3747.
(12) Fenter, F. F.; Caloz, F.; Rossi, M. J. *J. Phys. Chem.* **1994**, *98*, 9801.
(13) Beichert, P.; Finlayson-Pitts, B. J. *J. Phys. Chem.* **1996**, *100*, 15218.
(14) Leu, M.-T.; Timonen, R. S.; Keyser, L. F.; Yung, Y. L. *J. Phys. Chem.* **1995**, *99*, 13203.
(15) Schroeder, W. H.; Urone, P. *Environ. Sci. Technol.* **1974**, *8*, 756.
(16) Finlayson-Pitts, B. J. *Nature* **1983**, *306*, 676.
(17) Peters, S. J.; Ewing, G. E. *J. Phys. Chem.* **1996**, *100*, 14093.
(18) Langer, S.; Pemberton, R. S.; Finlayson-Pitts, B. J. *J. Phys. Chem. A* **1997**, *101*, 1277.
(19) Behnke, W.; Elend, M.; George, C.; Kruger, H.-U.; Scheer, V.; Zetzsch, C. Gas−Liquid Interactions. In *Heterogeneous and Liquid-Phase Processes*; Warneck, P., Ed.; Springer-Verlag: Heidelberg, 1996; pp 153−162.
(20) Livingston, F. E.; Finlayson-Pitts, B. J. *Geophys. Res. Lett.* **1991**, *18*, 17.
(21) George, Ch.; Ponche, J. L.; Mirabel, Ph.; Behnke, W.; Scheer, V.; Zetsch, C. *J. Phys. Chem.* **1994**, *98*, 8780.
(22) Fenter, F. F.; Caloz, F.; Rossi, M. J. *J. Phys. Chem.* **1996**, *100*, 1008.
(23) Zetzsch, C.; Behnke, W. *Ber. Bunsen-Ges. Phys. Chem.* **1992**, *96*, 488.
(24) Rudich, Y.; Talukdar, R. K.; Ravishankara, A. R.; Fox, R. W. *J. Geophys. Res.* **1996**, *101*, 21023.
(25) Vogt, R.; Crutzen, P. J.; Sander, R. *Nature* **1996**, *383*, 327.
(26) Sander, R.; Crutzen, P. J. *J. Geophys. Res.* **1996**, *101*, 9121.
(27) Abbatt, J. P. D. *Geophys. Res. Lett.* **1994**, *21*, 665.
(28) Abbatt, J. P. D. *J. Geophys. Res.* **1995**, *100*, 14009.
(29) Hanson, D. R.; Ravishankara, A. R. *Geophys. Res. Lett.* **1995**, *22*, 385.
(30) Allanic, A.; Oppliger, R.; Rossi, M. J. *J. Geophys. Res.* **1997**, *102*, 23529.
(31) Kirchner, U.; Benter, Th.; Schindler, R. N. *Ber. Bunsen-Ges. Phys. Chem.* **1997**, *101*, 975.
(32) Hu, J. H.; Abbatt, J. P. D. *J. Phys. Chem. A* **1997**, *101*, 871.
(33) Mozurkewich, M.; Calvert, J. G. *J. Geophys. Res.* **1988**, *93*, 15889.
(34) Van Doren, J. M.; Watson, L. R.; Davidovits, P.; Worsnop, D. R.; Zahniser, M.; Kolb, C. E. *J. Phys. Chem.* **1991**, *95*, 1684.

(35) Fried, A.; Henry, B. E.; Calvert, J. G.; Mozurkewich, M. *J. Geophys. Res.* **1994**, *99*, 3517.
(36) Hanson, D. R.; Lovejoy, E. R. *Geophys. Res. Lett.* **1994**, *21*, 2401.
(37) Lovejoy, E. R.; Hanson, D. R. *J. Phys. Chem.* **1995**, *99*, 2080.
(38) Zaytsev, I. D., Aseyev, G. G., Eds. *Properties of Aqueous Solutions*; CRC Press: New York, 1992; pp 635−641.
(39) Linke, W. F.; Seidell, A. *Solubilities, Inorganic and Metal-Organic Compounds*, 4th ed.; American Chemical Society: Washington, DC, 1965; pp 958−959.
(40) Bruins, A. P. *Mass Spectrom. Rev.* **1991**, *10*, 53.
(41) Huey, L. G.; Hanson, D. R.; Howard, C. J. *J. Phys. Chem.* **1995**, *99*, 5001.
(42) Brown, R. L. *J. Res. Natl. Bur. Stand. (U.S.)* **1978**, *83*, 1.
(43) Fuchs, N. A.; Sutugin, A. G. *Highly Dispersed Aerosols*; Ann Arbor Science: Ann Arbor, MI, 1970.
(44) Hirschfelder, J. O.; Curtiss, C. F.; Bird, R. B. *Molecular Theory of Gases and Liquids*; Wiley and Sons: New York, 1964.
(45) Barnes, R. J.; Lock, M.; Coleman, J.; Sinha, A. *J. Phys. Chem.* **1996**, *100*, 453.
(46) Oxtoby, D. W.; Nachtrieb, N. H. *Principles of Modern Chemistry*, 3rd ed.; Saunders College Publishing: New York, 1996; p 215.
(47) Kumar, K.; Margerum, D. W. *Inorg. Chem.* **1987**, *26*, 2706.
(48) Jolles, Z. E., Ed. *Bromine and its Compounds*; Academic Press: New York, 1966; p 155.
(49) Brimblecombe, P.; Clegg, S. L. *J. Atmos. Chem.* **1988**, *7*, 1.
(50) Winkler, P.; Junge, C. *J. Res. Atmos.* **1972**, *18*, 617.
(51) Tang, I. N.; Munkelwitz, H. R.; Davis, J. G. *J. Aerosol Sci.* **1977**, *8*, 149.
(52) Cziczo, D.; Hu, J. H.; Nowak, J. B.; Abbatt, J. P. D. *J. Geophys. Res.* **1997**, *102*, 18843.
(53) Dankwerts, P. V. *Gas−Liquid Reactions*; McGraw-Hill: New York, 1970.
(54) Hanson, D. R.; Lovejoy, E. R. *J. Phys. Chem.* **1996**, *100*, 6397.
(55) Blatchley, E. R.; Johnson, R. W.; Alleman, J. E.; McCoy, W. F. *Water Res.* **1992**, *26*, 99.
(56) This diffusion coefficient is taken to be the value measured for HBr in water at room temperature, as referenced in: Gray, D. E., Ed. *American Institute of Physics Handbook*, 3rd ed.; McGraw-Hill: New York, 1972; pp 2−223.
(57) Hanson, D. R.; Ravishankara, A. R.; Solomon, S. *J. Geophys. Res.* **1994**, *99*, 3615.
(58) Warneck, P. *Chemistry of the Natural Atmosphere*; Academic Press: San Diego, 1988; p 339.
(59) Yeatts, L. B.; Taube, H. *J. Am. Chem. Soc.* **1949**, *71*, 4100.
(60) The uptake coefficient γ^{O3} is calculated using eq 15 with parameters appropriate for the termolecular reaction between H^+, Cl^-, and O_3. In particular, the termolecular rate constant is 2.9×10^{-2} M^{-2} s^{-1},[59] and the Henry's law constant for O_3 is 1×10^{-2} M/atm.[61] D^{O3}, $[H^+]$, and $[Cl^-]$ were taken to be the values used in the γ^{HOBr} calculation.
(61) Seinfeld, J. H. *Atmospheric Chemistry and Physics of Air Pollution*; John Wiley and Sons: New York, 1986; p 199.
(62) For example: Zetzsch, C.; Pfahler, G.; Behnke, W. *J. Aerosol Sci.* **1988**, *19*, 1203.
(63) Oum, K. W.; Lakin, M. J.; DeHaan, D. O.; Brauers, T.; Finlayson-Pitts, B. J. *Science* **1998**, *279*, 74.